Improving the mechanical and biological functions of cell sheet constructs: The interplay of human-derived periodontal ligament stem cells, endothelial cells and plasma rich in growth factors

Eduardo Anitua [a,b,*], María Troya [a,b], Mar Zalduendo [a,b], Roberto Tierno [a,b], Mohammad H. Alkhraisat [a,b], Nerea Osinalde [c], Asier Fullaondo [b,d], Ana M. Zubiaga [b,d]

[a] *BTI-Biotechnology Institute, Vitoria, Spain*
[b] *University Institute for Regenerative Medicine & Oral Implantology, UIRMI (UPV/EHU-Fundación Eduardo Anitua), Vitoria, Spain*
[c] *Department of Biochemistry and Molecular Biology, Faculty of Pharmacy, University of the Basque Country (UPV/EHU), Vitoria-Gasteiz, Spain*
[d] *Department of Genetics, Physical Anthropology and Animal Physiology, University of the Basque Country (UPV/EHU), Leioa, Spain*

A B S T R A C T

Objective: The aim of this study was to produce and characterize triple-layered cell sheet constructs with varying cell compositions combined or not with the fibrin membrane scaffold obtained by the technology of Plasma Rich in Growth Factors (mPRGF).
Materials and methods: Human primary cultures of periodontal ligament stem cells (hPDLSCs) were isolated, and their stemness nature was evaluated. Three types of triple-layered composite constructs were generated, composed solely of hPDLSCs or combined with human umbilical vein endothelial cells (HUVECs), either as a sandwiched endothelial layer or as coculture sheets of both cell phenotypes. These three triple-layered constructs were also manufactured using mPRGF as cell sheets' support. Necrosis, glucose consumption, secretion of extracellular matrix proteins and synthesis of proangiogenic factors were determined. Histological evaluations and proteomic analyses were also performed.
Results: The inclusion of HUVECs did not clearly improve the properties of the multilayered constructs and yet hindered their optimal conformation. The presence of mPRGF prevented the shrinkage of cell sheets, stimulated the metabolic activity and increased the matrix synthesis. At the proteome level, mPRGF conferred a dramatic advantage to the hPDLSC constructs in their ability to provide a suitable environment for tissue regeneration by inducing the expression of proteins necessary for bone morphogenesis and cellular proliferation.
Conclusions: hPDLSCs' triple-layer construct onto mPRGF emerges as the optimal structure for its use in regenerative therapeutics.
Clinical relevance: These results suggest the suitability of mPRGF as a promising tool to support cell sheet formation by improving their handling and biological functions.

1. INTRODUCTION

Cell-based therapies, regenerative medicine, and tissue engineering have rapidly evolved in recent years. The latter combines the use of cells, scaffolds, and biological cues to restore the functionality of damaged tissues. However, several drawbacks such as inflammation, autoimmunity, impaired nutrient diffusion, high rate of cell death, low cell seeding density, uneven cell distribution or excessive connective tissue formation have been associated with the use of these types of structures in conventional tissue engineering [1–4]. Cell Sheet Technology (CST) has

been proposed as an alternative approach to overcome the traditional scaffolds' shortcomings regarding regenerative therapies [5]. In fact, this technology has already been applied for the reparation and regeneration of several tissues including heart, cornea, lung, periodontium, esophagus and cartilage [1,6,7]. Cell sheets can be transplanted directly into the target tissue or even used to create three-dimensional (3D) tissue-like structures in order to repair and regenerate organs with more complex structures. An attractive property of cell sheets is that they preserve cell-cell interactions and extracellular matrix (ECM) that characterize cellular microenvironments, which are crucial for cell

functions. Consequently, cell sheet engineering has emerged as a promising cell-based therapy that can be applied in a wide range of regenerative treatments and biomedical modelling strategies [8]. This approach exhibits numerous advantages over conventional regenerative therapies, including their higher cell survival rate and biocompatibility [9], strong adhesion [10], a greater control over the structure and composition of the formed tissues [11], the absence of limitations associated with scaffold degradation [1], a higher control over immunity and immunogenicity [12], and the possibility of incorporating specific structures that mimic the complex architecture of native tissues [2].

Cell sheets are noninvasively harvested without the use of proteolytic enzymes, thus thoroughly preserving cell-cell junctions and ECM components [1,13]. Consequently, the constructed tissues exhibit high cell densities and improved adhesiveness, thus providing an efficient local administration of cells and increasing overall viability [2,14]. 3D constructs can be manufactured by simply stacking the cell sheets to mimic physiological tissues more closely, free from the inherent constraints of scaffolds [1,14,15]. Different systems can be used to obtain cell sheets, including temperature-responsive, electro-responsive, pH-responsive, mechanical, and magnetic systems [2]. The thermo-responsive polymer poly (N-isopropylacrylamide) (PIPAAm) is the most well-known and widely used molecule in this field to coat culture dishes [16]. It undergoes a conformational transformation in response to temperature changes, which modifies its chemical properties oscillating between hydrophobicity and hydrophilicity. Simply modifying this parameter enables the control of cell adhesion and detachment. When the incubation temperature is around 20 ºC, PIPAAm becomes hydrophilic, and the cell sheet detaches spontaneously [15–17].

For a successful tissue engineering approach based on cell sheet technology, a number of variables need to be considered, including the source of cells and nutrient availability. Mesenchymal stem cells (MSCs) are increasingly being considered as suitable candidates for cell-based engineering approaches due to their extensive expansion rate and potential to differentiate into other mesodermal origin lineages [18–20]. In this sense, the human periodontal ligament stem cells (hPDLSCs) are an easily accessible source of stem cells that possess similar properties to MSCs [21,22]. Regarding nutrient availability, the lack of blood vessels in engineered tissues can lead to improper cell integration, thereby preventing nutrient diffusion or even facilitating cell necrosis [23,24]. Consequently, the inclusion of the endothelial cell phenotype into multi-layered constructs has been described to improve the prevascular network in 3D constructs, either as a sheet sandwiched between two layers of mesenchymal precursor cells or as sheets made as cocultures of hPDLSCs and endothelial cells [17,25].

Nevertheless, the weak mechanical properties of the multi-layered constructs constitute an important limitation of this technology that prevents their use as scaffold-free constructs [2,3]. The combination of cell sheet multi-layered constructs with the fibrin membrane obtained via Plasma Rich in Growth Factors (mPRGF) technology could be considered a promising strategy to overcome physical restrictions. This combination has been proposed as a better choice than conventional tissue engineering in which cell suspensions are used and cell-cell junctions and ECM have been lost [2].Fibrin is a versatile scaffold that has been widely used in wound healing and tissue repair as it constitutes the natural provisional matrix that includes many cell and ECM binding sites, thus providing not only physical support, but also biological signals that regulate cell fate and behaviour [26,27]. In particular, the scientific evidence strongly supports that PRGF based membranes enhance *in vitro* cell proliferation [28] and reduce oxidative stress [29], while promoting extracellular matrix biosynthesis and fibrinolysis simultaneously [30]. Moreover, PRGF membranes also improved chemically induced lesions in a rabbit alkali-burn model [31]. *In vivo* clinical trials have revealed that PRGF fibrin membranes accelerate ocular surface regeneration, thus minimizing inflammation and fibrosis after glaucoma filtering and ocular surface surgery [32,33].

The aim of this study was to produce triple-layered cell sheet constructs with varying cell compositions on temperature-responsive dishes and analyze their properties in the presence or absence of a fibrin scaffold. Cell sheets were prepared either exclusively with PDLSCs or in combinations with Human Umbilical Vein Endothelial Cells (HUVECs), depending on the model structure. In addition, the same types of triple-layered constructs were manufactured using PRGF fibrin membranes (mPRGF) as cell sheet support. Importantly, PRGF was also used as culture medium supplement instead of xenogeneic fetal bovine serum (FBS) for the generation and culture of the constructs. As a result, a total of six models were assessed for their suitability in a successful tissue regeneration, by examining features such as angiogenesis, metabolic activity, ECM secretion and necrosis. Quantitative proteomic analysis completed the characterization of triple-layered cell sheet constructs.

2. Material & Methods

The study was performed following the principles established in the Declaration of Helsinki amended in 2013 and in accordance with the ethical standards from the Araba University Hospital Clinical Research Ethical Committee (BTI-01-IV/02/20/CST).

2.1. Preparation of plasma rich in growth factors (PRGF)

In order to obtain the PRGF supernatant for culture medium supplementation, blood from 3 healthy donors was collected into tubes with 3.8 % (wt/v) sodium citrate after written informed consent was provided. Blood was then centrifuged at 580 *g* for 8 min at room temperature (RT) (Endoret System; BTI Biotechnology Institute, S.L., Miñano, Álava, Spain). The whole plasma column, avoiding the buffy coat, was pooled from all the donors to obtain the plasma rich in growth factors (PRGF). Plasma preparation was activated with calcium chloride following the manufacturer's instructions. After 1 h, the PRGF clot was centrifuged at 1000 g for 10 min at RT. Finally, the supernatant was filtered, aliquoted and stored at −80 ºC for its subsequent use and replaced the FBS for maintenance of cell sheets and triple-layer-constructs.

2.2. Preparation of the fibrin membrane from PRGF (mPRGF)

The whole plasma column (PRGF) was collected from one healthy donor's blood, as described above. For obtaining a PRGF fibrin membrane matching the size of a well of 6-well plates, 4 mL of PRGF were activated in 5-mL rootstock containers (BTI Biotechnology Institute). Subsequently, the clot was transferred to a fibrin membrane shaper (BTI Biotechnology Institute) and the fibrin membrane was obtained after compressing for 5 min [34].

2.3. Cell isolation and culture

Human primary cultures of periodontal ligament stem cells were obtained from one healthy 18-year-old patient who underwent a simple extraction of a non-impacted wisdom tooth and after written informed consent was signed. Cells were isolated by the explant method [35]. Briefly, the tooth was rinsed in phosphate-buffered saline (PBS) containing 50 µg/mL gentamicin and 2.5 µg/mL amphotericin B (both from Sigma-Aldrich Inc., St. Louis, MO, USA). Periodontal ligament was then removed from the middle third of the tooth roots using a scalpel, and minced into smaller portions. The pieces of tissue were placed into 6-well plates and cultured in Dulbecco's modified Eagle's medium (D-MEM)/F-12 (1:1 vol) with 2 mM glutamine (both from Gibco-Invitrogen, Grand Island, NY, USA), 50 µg/mL gentamicin and 2.5 µg/mL amphotericin B and 10 % FBS (Biochrom AG, Leonorenstr, Berlin, Germany) at 37 ºC in a humidified 5 % CO_2 atmosphere. Culture medium was changed every 3–4 days. After reaching subconfluence, cells were detached with TrypLE Select (Gibco-Invitrogen) and

subcultured. Cell viability was assessed by trypan blue dye (Sigma-Aldrich Inc.) exclusion. Cells between 3rd and 7th passages were used in the experiments. FBS was replaced by PRGF supernatant in the culture medium without amphotericin B (hereafter routine culture medium) for cell amplification and characterization, and triple-layered cell construct maintenance.

Human Umbilical Vein Endothelial Cells (HUVEC) (Lonza Group Ltd, Basel, Switzerland) were cultured in endothelial growth medium (EGM) (ScienCell Research Laboratories Inc., Carlsbad, CA, USA), which consisted of endothelial basal medium supplemented with penicillin/streptomycin solution, endothelial cell growth supplements and 5 % PRGF supernatant. They were maintained following the supplier's instructions.

2.4. Characterization of hPDLSCs

2.4.1. Cell surface antigen expression
hPDLSCs were analyzed for mesenchymal stem cell surface antigen expression by flow cytometry following the standard criteria established by the International Society for Cell and Gene Therapy (ISCT) [36]. Antibodies against CD73, CD90, CD14, CD19, CD45 and IgG1 (FITC-conjugated), CD105, CD34 and IgG1 (APC-conjugated) and HLA-DR and IgG2a (PE-Cy5- conjugated) (all provided by Becton, Dickinson and Company, Franklin Lakes, NJ, USA) were used, and 2.5×10^5 cells were analyzed per antibody. After the washing and blocking steps, samples were incubated for 1 h at 4 °C protected from light. Following the incubation, samples were washed, fixed in 1 % paraformaldehyde and finally analyzed by a Gallios flow cytometer (Beckman-Coulter, High Wycombe, Buckinghamshire, UK) [37].

2.5. Colony forming unit assay

Clonogenic potential was assessed by means of the colony forming unit assay. Cells were seeded on 6-well plates at a density of 50 cells/cm^2 in routine culture medium. Medium was changed every 3–4 days. After 7 days, cells were washed with PBS and stained with 1 % crystal violet (Prolab Diagnostics, ON, Canada) in methanol for 30 min. Finally, cells were washed with ultrapure water to remove excess of stain and colonies containing more than 50 cells (>2 mm) were examined under an inverted light microscope (Leica DM IRB) (Leica Microsystems, Wetzlar Hesse, Germany).

2.6. Osteogenic differentiation

The osteogenic differentiation capacity of hPDLSCs was evaluated. A total of 10000 cells/cm^2 were seeded onto 48-well plates in routine culture medium. After reaching 50–70 % confluence, medium was replaced by the differentiation medium supplied in the human mesenchymal stem cell functional identification kit (R&D Systems Inc), and the manufacturer's instructions were followed. Cells cultured with the routine culture medium were used as negative control. Media were renewed twice a week. After 4 weeks of culture, osteogenic differentiation was assessed by the alizarin red staining of calcium deposits. Briefly, cells were washed with PBS and fixed with 4% paraformaldehyde for 30 min at RT. After fixation, they were washed twice with ultrapure water and stained with 1.4 % alizarin red solution (pH = 4.1) (Merck KGaA, Darmstadt, Germany) for 5 min at RT. Cells were then washed again with ultrapure water and finally cell cultures were observed under an inverted light microscope (Leica DM IRB).

2.7. Adipogenic differentiation

For adipogenic differentiation, hPDLSCs were seeded on 48-well plates at a density of 15000 cells/cm^2 in routine culture medium. After reaching 100 % confluence, medium was replaced by the differentiation medium supplied in the human mesenchymal stem cell functional identification kit (R&D Systems Inc., Minneapolis, MN, USA). Cells cultured with the routine culture medium were used as negative control. Media were changed every 3–4 days. After 5 weeks, adipogenic differentiation was confirmed by the detection of intracellular accumulation of neutral lipids with the HCS LipidTOX (Millipore Corporation, Burlington, MA, USA.) red staining. Briefly, cells were fixed with 4 % paraformaldehyde and incubated with LipidTox solution (1:100) for 30 min. Finally, cell nuclei were counterstained with Hoechst.

2.8. Fabrication of triple-layered cell constructs

Three types of multi-layered constructs and 6 replicates of each were performed. After collecting the conditioned culture media for quantification of several molecules, half of the constructs were used for histologic examination and the other half for proteomic analysis.

2.8.1. Triple-layered composite construct of hPDLSCs: hPDLSCs / hPDLSCs / hPDLSCs (PPP)
hPDLSCs were seeded on 6-well Nunc UpCell temperature-responsive plates (ThermoFisher Scientific Inc, Waltham, MA, USA) at a density of 10,000 cells/cm^2 in the hPDLSC routine culture medium. Cells were maintained under normal culture conditions (37 °C in a humidified 5 % CO$_2$ atmosphere) until confluent cultures were observed. hPDLSCs were then incubated at 20 °C and allowed to detach spontaneously from the culture plate and to float in the culture medium as monolayer cell sheets (Fig. 1, A and B). Cell sheets significantly shrank upon the process of detaching, where cytoskeletal reorganization occurs. In parallel, the recipient wells for the cell sheets were incubated with PRGF supernatant for 30 min to improve the adhesion of the first cell sheet of the construct. Cell sheets were aspirated and transferred to these receiving wells after removing PRGF (Fig. 1C). Plates were then maintained at 37 °C, after removing most of the volume of medium. Subsequently, another confluent plate with hPDLSCs was similarly processed to obtain the 2nd cell sheet, which was placed onto the first one (Fig. 1D). The process was repeated once more to add the 3rd layer to successfully prepare the triple-layered cell structures (Fig. 1E). These constructs were incubated under normal conditions for 1 h and with a scarce volume of culture medium to allow both the complete attachment among the cell sheets and also to the plate surface. After that, 1.5 mL of culture medium was added to each well.

2.8.2. Triple-layered composite construct with sandwiched endothelial cells: hPDLSCs / HUVEC / hPDLSCs (PHP)
Two different cell phenotypes were included in this type of construct: primary hPDLSCs and HUVECs. The process for obtaining the multi-layered construct was similar to that described above. Briefly, hPDLSCs were seeded on 6-well temperature-responsive plates at a density of 10000 cells/cm^2 in routine culture medium. The 6-well temperature-responsive plates used for HUVECs were previously coated with 0.1 % Gelatin Solution (Merck KGaA). Endothelial cells were seeded at a density of 6000 cells/cm^2 in EGM. When both cultures reached confluence, hPDLSCs were incubated at 20 °C to be detached as a cell sheet. In parallel, the recipient wells were coated with PRGF supernatant, as explained before. The detached cell sheets were then aspirated and transferred to these receiving wells, where they were kept at 37 °C. In parallel, HUVECs were also incubated at 20 °C. In this case, the cell monolayer was not detached as a whole but fragmented. Pieces of the cell sheet were collected and centrifuged at 220 g for 5 min. After discarding the supernatant, the pellet was resuspended in 5 μL of EGM to be distributed onto the first hPDLSCs sheet in the receiving wells. These two-layer constructs were incubated at 37 °C for 30 min to promote the settlement of the endothelial cells on the hPDLSCs sheet. Finally, the last hPDLSCs sheet was obtained and placed coating HUVECs' layer, thus resulting in a construct that consisted of a layer of endothelial cells inserted between a double layer of ligament stem cells. These sandwich constructs were incubated at 37 °C with a sparse volume of culture
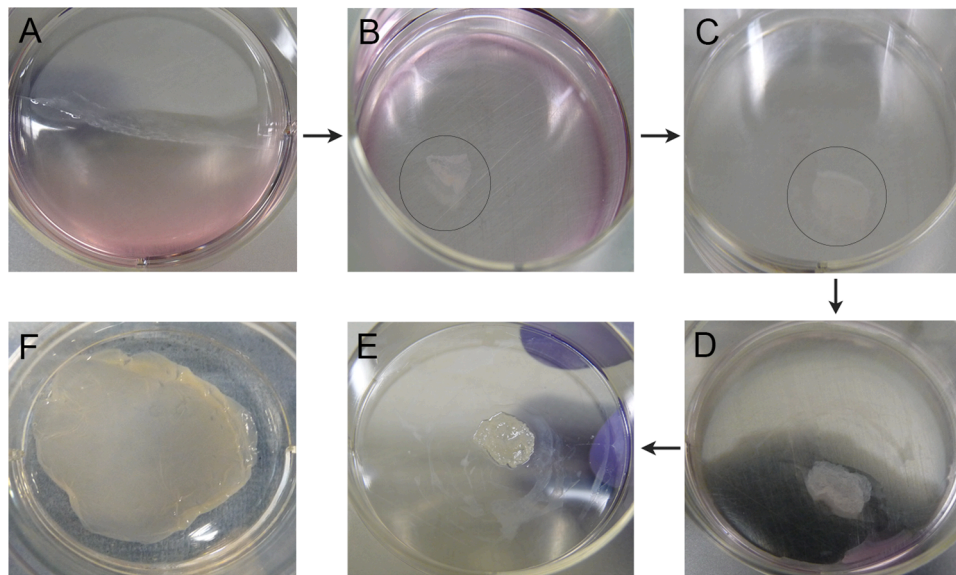
Fig. 1. Macroscopic photograph gallery illustrating the process of generating triple-layered cell constructs. A) Spontaneous detachment of a cell monolayer onto a temperature-responsive well plate after maintaining it at 20 ºC. B) Shrinkage and floating of the cell sheet. C) Cell sheet transfer onto another well, previously coated with PRGF or gelatin solution depending on the trilaminar cell composite, in scarcely volume of culture medium. D) Two-layer and E) three-layer construct generation after repeating this process 1 and 2 times, respectively. F) Avoiding of cell sheet shrinkage when mPRGF was used as a cell monolayer support for triple-layered constructs fabrication.

medium to facilitate adhesion. After 1 h, 1.5 mL of a mixture of the culture media of both cell phenotypes at a ratio of 1:3 was added (hPDLSCs' routine culture medium: EGM).

2.8.3. Triple-layered composite construct of cocultures of hPDLSCs and HUVEC: hPDLSCs + HUVEC / hPDLSCs + HUVEC / hPDLSCs + HUVEC (3PH)

hPDLSCs and HUVECs were also included in this type of construct, but in this case the three cell sheets were identical, composed of co-cultures of both cell types. For preparing a coculture sheet, hPDLSCs and HUVECs were seeded at a 1:1 ratio into the same well of a 6-well temperature-responsive plate, previously coated with 0.1 % Gelatin Solution. The seeding density for both cell types was 5000 cells/cm². Cultures were maintained with a mixture of the hPDLSC routine culture medium and EGM at a ratio of 1:3. The cultures were incubated at 37 ºC until reaching confluence. Monolayers that would be the bottom layers of the construct were obtained after incubating at 20 ºC, as described above for hPDLSC sheets. Meanwhile, the receiving wells were incubated with 0.1 % Gelatin Solution. The first cell coculture sheet was then transferred to these receiving wells and maintained with a small volume of the culture media mixture under normal culture conditions to allow cell sheet attachment. The process was repeated for another two layers, and cell coculture sheets were placed on top of each other to complete the triple-layered construct. Finally, 1.5 mL of culture media mixture at a ratio of 1:3 was added.

2.9. Fabrication of triple-layered cell constructs onto the mPRGF

The seeding and culture of both hPDLSC and HUVEC cell types for obtaining cell sheets were performed similarly to what is described above for the three types of fibrin-free multi-layered constructs. The main difference was that in this case, the mPRGF was carefully placed onto the first confluent monolayer, that is, the one at the bottom of the construct, before incubating them at 20 ºC. After 45 min, mPRGF together with the cell sheet adhered underneath was detached from the culture dish and transferred onto another confluent monolayer so that the 2 cell sheets were now in contact with each other. This process was repeated once more with the third cell sheet. Finally, the triple-layered

cell constructs with the mPRGF were turned over, so that the cell sheets were facing up, and transferred to another well (Fig. 1F). Just like the constructs without mPRGF, 8 replicates of each type were assigned for histologic, proteomic and quantification analysis. Finally, 1.5 mL of the corresponding culture medium was added to the wells. Therefore, using the mPRGF as cell sheet support, the 3 models of triple-layered cell constructs were obtained.

2.10. Proteomic Analysis

2.10.1. Sample preparation and TMT labeling

Triple-layered composite constructs without mPRGF were washed with PBS for 3 times and collected into microtubes. After centrifuging them at 500 g for 7 min, the supernatant was discarded, and pelleted cell structures were stored at −80 ºC until their analysis. When mPRGF was included in the triple-layered constructs, the fibrin membrane was removed to avoid any interference in the proteomic analysis. Therefore, after washing with PBS, these construct models were incubated in Tryple solution for 1 h. Subsequently, a cell scrapper was used to dissociate the cells from the fibrin membrane and cell suspensions were filtrated through a 70 μm filter and then centrifuged. Cell pellets were washed 3 times in PBS and were stored dry at −80 ºC until their analysis.

For homogenization, the cell pellet (≈3e5 cells) was resuspended in ST lysis solution (0.1 M Tris-HCl pH 7.6, 4 % SDS) at a ratio of 20 μl ST/1e5 cells. The homogenate was sonicated for 3 min, heated at 95 ºC for 5 min, centrifuged at 16,000g for 10 min and the supernatant was collected. The amount of total protein in the supernatant was determined using the Pierce bicinchoninic acid (BCA) Protein Assay Kit (ThermoFisher Scientific Inc).

75 μg of total protein was subjected to tryptic digestion. For protein reduction, dithiothreitol (DTT) was added to the samples at a final concentration of 100 mM and incubated at 60 ºC for 30 min. Digestion was performed following the protocol described by Wisniewski et al. [38] on Amicon Ultra-0.5 mL Centrifugal Filter Unit (30 kDa) (Merck KGaA) devices. Briefly, filters were centrifuged at 14,000g for 15 min at 20 ºC and the following dilution-concentration cycles were performed with UA buffer (100 mM Tris-HCl pH 8. 5, 8 M urea) and AMBIK buffer (50 mM NH4HCO3): 200 μl UA (2X), 100 μl of 50 mM iodoacetamide in

UA (incubate 30 min in the dark), 200 µl UA (3X), 100 µl AMBIK (3X). Finally, 40 µL of trypsin (F. Hoffman-La Roche Ltd, Wurmisweg, Kaiseraugst, Switzerland) in AMBIK was added at a 50:1 protein enzyme ratio. Samples were incubated at 37 °C for 16 h and tryptic peptides were collected by centrifugation and subsequent washing of the filters with 50 µL of AMBIK. The resulting filtrates were desalted using Sep-Pak C18 Cartridge columns (Waters Corporation, Milford, MA. USA) and dried in a SpeedVac (ThermoFisher Scientific Inc) vacuum concentrator.

Prior to isobaric labeling the samples were resuspended in 50 mM triethylammonium bicarbonate buffer (TEAB) and total peptide concentration was determined using the Pierce Quantitative Fluorometric Peptide Assay kit (ThermoFisher Scientific Inc). Between 10 and 15 µg of peptides were labeled using the TMT10plex Mass Tag Labeling Kit (ThermoFisher Scientific Inc) following the manufacturer's instructions. After TMT labeling, all samples were mixed at a 1:1 ratio, dried in a SpeedVac (ThermoFisher Scientific Inc) vacuum concentrator and fractionated using the Pierce High pH Reversed-Phase Peptide Fractionation Kit (ThermoFisher Scientific Inc) according to the manufacturer's instructions.

2.11. Liquid chromatography-mass spectrometry (LC-MS/MS)

LC-MS/MS analyses were performed on a Q Exactive HF-X ((ThermoFisher Scientific Inc)) (w/o mPRGF) and an Exploris 480 (with mPRGF) mass spectrometer (ThermoFisher Scientific Inc) coupled to an Easy-nLC 1200 nanoUPLC System (ThermoFisher Scientific Inc) via a Nanospray Flex Ion Source ionization source (ThermoFisher Scientific Inc). Peptides were resuspended in 0.1 % formic acid and loaded onto an Acclaim PepMap100 precolumn (ThermoFisher Scientific Inc) (75 µm x 2 cm), connected to an Acclaim PepMap RSLC analytical column (ThermoFisher Scientific Inc) (50 µm x 25 cm) (ThermoFisher Scientific Inc). Samples w/o mPRGF were analysed in the Q Exactive HF-X mass spectrometer. Peptides were eluted at a flow rate of 300 nl/min with the following percentage of acetonitrile in 0.1 % formic acid: 150 min 2–24 %, 2 min 24–32 %, 1 min 32–80 %, 12 min 80 %. Q Exactive HF-X mass spectrometer was operated in data dependent acquisition (DDA) mode. Full MS scans were acquired from m/z 375–1800 with a resolution of 60,000 at m/z 200. The 10 most intense ions were fragmented by higher energy C-trap dissociation with a stepped normalized collision energy of 28 and 32. MS/MS spectra were recorded with a resolution of 45,000 at m/z 200. The maximum ion injection time was 50 ms for survey scans and 100 ms for MS/MS scans, whereas automatic gain control (AGC) target values of 3×10^6 and 1×10^5 were used for survey and MS/MS scans, respectively. A dynamic exclusion time of 20 s was applied and singly charged ions, ions with 6 or more charges, and ions with unassigned charge state were excluded from MS/MS. Samples with mPRGF were analyzed in the Exploris 480 mass spectrometer. Peptides were eluted at a flow rate of 300 nl/min with the following percentage of acetonitrile in 0.1 % formic acid: 96 min 0–15 %, 35 min 15–24 %, 22 min 24–32 %, 3 min 32–76 %, 10 min 76 %. The mass spectrometer was operated in data dependent acquisition (DDA) mode in a 3 second cycle time. Full MS scans were acquired from m/z 350–1600 with a resolution of 60,000 at m/z 200. Ions were fragmented by higher energy C-trap dissociation with a normalized collision energy of 36 %. MS/MS spectra were recorded with a resolution of 45,000 at m/z 200. The maximum ion injection time was set to 50 ms for survey scans and auto for MS/MS scans, whereas normalized AGC target values of 300 % were used for both survey and MS/MS scans. A dynamic exclusion time of 40 s was applied and singly charged ions, ions with 6 or more charges, and ions with unassigned charge state were excluded from MS/MS. Data were acquired in both instruments using Xcalibur software (Thermo-Fisher Scientific Inc).

2.12. Proteomic data processing and analysis

Raw data files were processed with the MaxQuant software (version

1.6.17.0) [39] using the internal search engine Andromeda. Data originated from the different high pH fractions of the same samples were combined and searched against the UniProtKB-SwissProt database restricted to *Homo sapiens* proteins (version 2020_01). Mass tolerance was set at 8 and 20 ppm at MS and MS/MS level respectively. Enzyme specificity was set to trypsin and a maximum of 2 missed cleavages were allowed. Carbamidomethylation of C was selected as fixed modification and oxidation of M, protein N-terminal acetylation and deamidation of N and Q as variable modifications. Batch specific TMT correction factors were added based on manufacturer's product data sheet. False discovery rate (FDR) was set at 1 % at protein and peptide levels.

MS-derived data were analyzed using Perseus software v1.5.6 [40]. Data were filtered out for potential contaminants, for proteins identified in the decoy database, and for proteins only identified by site. The log2 transformed intensities were normalized to the median of each sample. The standard two-sided Student's t-test was applied to test for differences in protein abundance. Differential regulation threshold was set to log2-fold changes below −0.7 and above 0.7 with p-values below 0.05.

2.13. Gene Ontology (GO) analysis

To identify the statistically overrepresented GO biological processes, proteomic data were subjected to functional enrichment analyses using the ShinyGO v0.77 tool [41]. The ShinyGO parameters considered were p-value cutoff, FDR (0.05), species (*Homo sapiens)*, and minimum protein number in the pathway (34). The compilation of all the proteins detected by the proteomics experiment were established as the background proteome of the study. Venn diagrams were made using Jvenn [42].

2.14. Detection of necrosis and glucose consumption

The 6 models of triple-layered cell constructs were cultured for 48 h. Subsequently, conditioned media were collected, centrifuged at 500 g for 10 min, divided into aliquots and stored at −80 ºC until assay. The activity of lactate dehydrogenase (LDH) enzyme, widely used as a marker of cell death, was measured as LDH-reduced NADH (Abcam, Cambridge, UK). The amount of total glucose in the conditioned media by the constructs was quantified as a measure of metabolic activity to obtain energy (Cell Biolabs Inc, San Diego, CA, USA).

PRGF membranes without triple-layered cell constructs were also incubated in both types of culture media for 48 h and conditioned media were processed similarly and were used to subtract the background. Absorbances were measured with a Synergy H1 multimode microplate reader (Agilent-Biotek, Santa Clara, CA, USA).

2.15. Quantification of biomolecules in the culture medium

The conditioned media of triple-layered cell constructs collected after 48 h were also used to perform Enzyme-Linked Immunosorbent Assays (ELISA) in order to quantify the secretion of ECM proteins such as type I procollagen (Abcam) and fibronectin (Cell Biolabs Inc), and the presence of the cell adhesion molecule Integrin alpha 2 (ITG-α2) (Abyntek Biopharma SL, Derio, Bizkaia, Spain). The levels of the Vascular Endothelial Growth Factor (VEGF) and Stromal Cell Derived Factor-1 (SDF-1α) pro-angiogenic factors were also determined (both provided by ThermoFisher Scientific Inc). The background values were obtained and subtracted as described above.

2.16. Histological analysis

After 48 h of incubation, all types of constructs were fixed in neutral buffered formalin (Bio-Optica Milano, Milan, Italy) for 24 h, dehydrated with graded ethanol, cleared in pure xylene, paraffin-embedded and sectioned into slices about 5 µm in thickness (FFPE sections) using a rotary microtome RM2255 (Leica Biosystems, Wetzlar Hesse, Germany).

Histological slices were stained with Harris Haematoxylin and alcoholic Eosin Y solution (Sigma-Aldrich Inc.) to evaluate the cell distribution, structural integrity, density, and other morphological characteristics of the triple-layered cell constructs assayed. Chromogenic detection of collagen type I and CD31 (both from ABCAM) in FFPE sections was performed via immunohistochemistry based on streptavidin-biotin complex with DAB peroxidase (Vector Laboratories Inc., Burlingame, CA, USA) and 10 % v/v diluted Harris Haematoxylin as nuclear counterstain. Apoptosis was assessed by the terminal deoxynucleotidyl transferase dUTP-digoxigenin nick end labelling (TUNEL) method using the ApopTag peroxidase *in situ* detection kit (Merck KGaA).

2.17. Statistical analysis

Results were expressed as mean ± standard deviation. Shapiro-Wilk and Levene tests were performed to assess the parametric statistical assumptions of normality and homoscedasticity, respectively. When the populations were normal and the variances were homogeneous, Anova
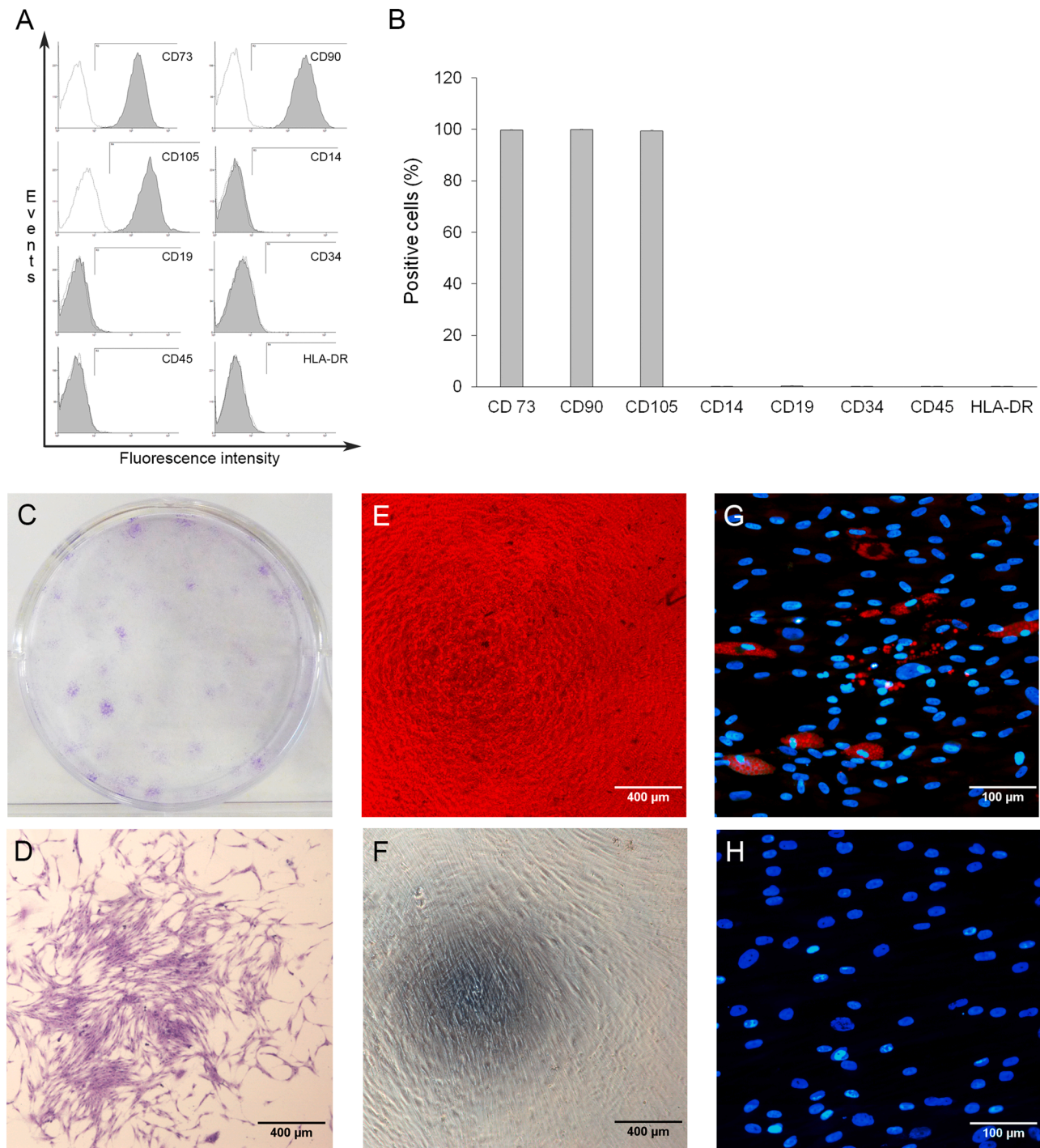
Fig. 2. Assessment of hPDLSC stemness. A) and B) Flow cytometric assay confirming the mesenchymal surface markers expression. CD73, CD90, CD105, CD14, CD19, CD34, CD45 and HLA-DR antigens were analysed. C) Crystal violet staining of colonies showing their clonogenic potential. D) Cluster of more than 50 cells considered as a colony. E) Photomicrographs of osteogenic differentiated and F) control cells after alizarin red staining. G) Detection of intracellular neutral lipids with LipidTOX red staining after adipogenic differentiation. Nuclei were counterstained with Hoechst. H) Only nuclei appeared stained in non-induced cells.

and Tukey post-hoc tests were performed. In the case of non-homogeneous variances but normal distribution, the non-parametric Kruskal Wallis test and the 2-tail t-test were performed, otherwise, a Mann Whitney test was used. All statistical analyses were performed using SPSS v23 (SPSS Inc., Chicago, IL, USA), being set the level of statistical significance as p<0.05.

3. Results

3.1. Characterization of hPDLSCs

3.1.1. Cell surface antigen expression

Flow cytometric analysis showed the expression of CD73, CD90 and CD105 antigens on the surface of more than 99 % of the hPDLSCs. In addition, no expression (<0.2 %) of CD14, CD19, CD34, CD45 and HLA-DR markers was detected (Fig. 2, A and B). According to the standard criteria established by the ISCT, these results confirmed the mesenchymal nature of the hPDLSCs culture.

3.2. Colony forming unit assay

To assess the clonogenic capacity of hPDLSCs, the colony forming unit assay was performed. Crystal violet staining revealed the ability of hPDLSC cells to form colonies, which were considered to be clusters of more than 50 cells (Fig. 2, C and D).

3.3. Cell differentiation

hPDLSCs maintained in differentiating culture media showed their ability to differentiate into both osteogenic and adipogenic lineages. Regarding osteogenic differentiation, the extracellular matrix mineralization after 4 weeks of treatment was confirmed by the alizarin red S staining (Fig. 2E). Moreover, the neutral lipid stain LipidTox revealed the formation of cytoplasmic lipid droplets after 35 days of treatment with the adipogenic inducers (Fig. 2G). Cells cultured in the routine culture medium included in both assays were negative for the aforementioned stains (Fig. 2, F and H).

3.4. Proteomic analysis

We aimed to study and compare the proteomic profile of triple-layered constructs composed by (i) solely hPDLSCs (PPP), (ii) sandwiched endothelial cells hPDLSCs/HUVEC/hPDLSCs (PHP) and (iii) hPDLSCs/HUVEC cocultures (3PH). All three constructs were cultured in the absence or presence of a fibrin membrane (mPRGF). For that purpose, two TMT-based quantitative proteomic analyses were carried out.

At least three biological replicates of each type of construct were analyzed and a total of 5557 (w/o mPRGF) and 6247 (with mPRGF) proteins were confidently identified and quantified. Principal components analysis (PCA) confirmed that the proteomes of the three types of constructs (PPP, 3PH and PHP) cultured either in the absence (Fig. 3A)
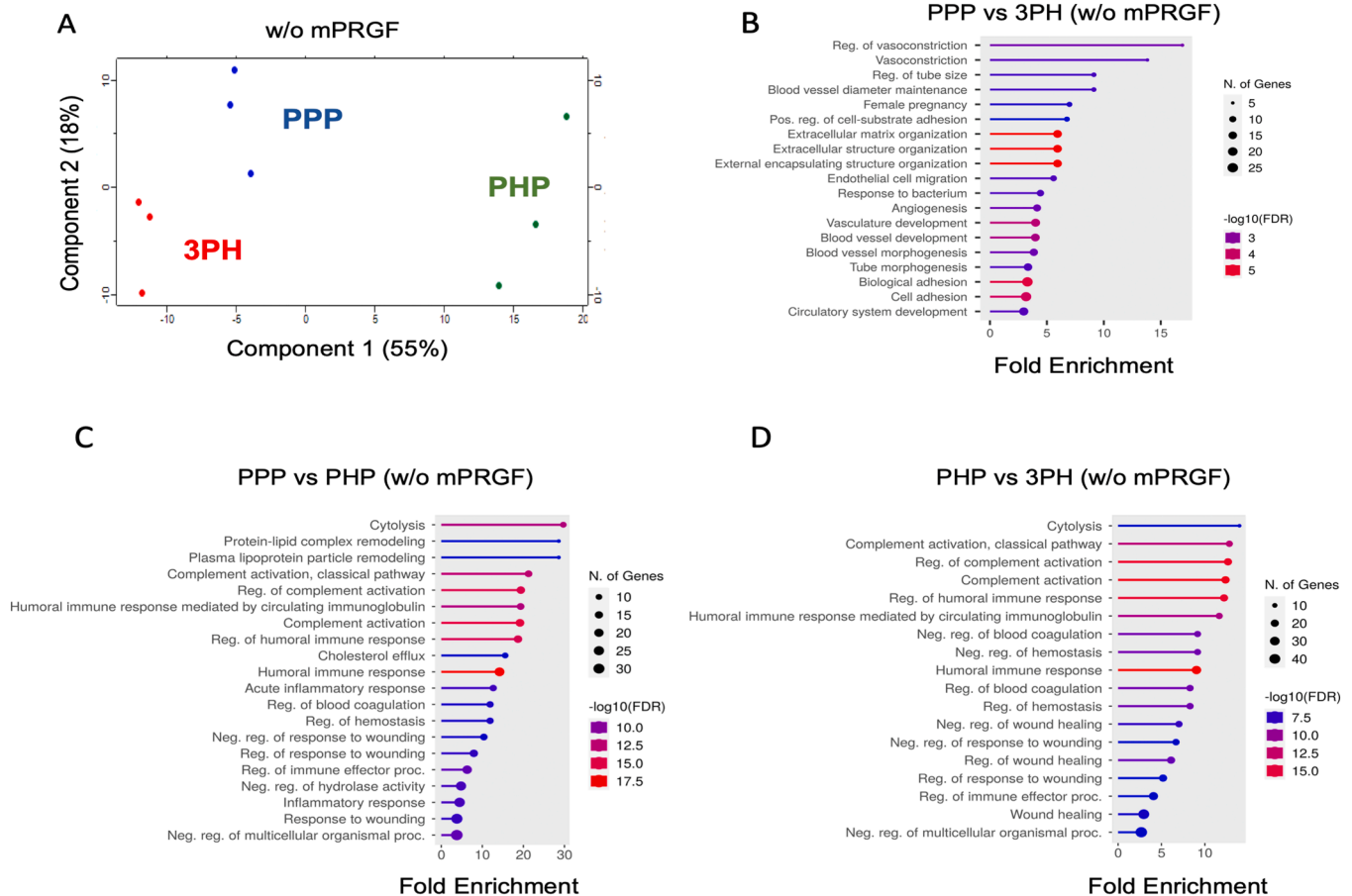
Fig. 3. Proteomic analysis of the triple-layered constructs without mPRGF. A) Principal component analysis (PCA) of proteomics data (Log2 fold changes) obtained in triple-layered constructs (n = 3). The PCA plot represents 5761 proteins with biological replicates that indicate proteomics profile differences between triple-layered constructs. B, C, D) Results of the GO enrichment analysis performed with the ShinyGO application, using as a background the total number of proteins identified in each of the comparisons. Shown are the number of differentially expressed proteins as spots belonging to top hallmark pathways. The spot size represents the number of differentially expressed proteins and spot color indicates enrichment confidence (FDR). X-axis denotes the enrichment factor of differentially expressed proteins.

or presence of a fibrin membrane (mPRGF) (Fig. 4A) were clearly different from each other.

In order to detect the proteins differentially expressed between the constructs generated, three types of comparisons were carried out (PPP *vs.* 3PH, PPP *vs.* PHP and PHP *vs.* 3PH) for each culture condition (± mPRGF). For each comparison, a volcano plot was generated highlighting in red significantly upregulated (log2 fold change > 0.7; p-value < 0.05) and in blue significantly downregulated (log2 fold change < −0.7; p-value < 0.05) proteins (Fig. 5). Differentially expressed proteins were considered for further analysis.

Regarding constructs cultured in the absence of the fibrin membrane

(w/o mPRGF), gene ontology (GO) enrichment analysis of the differentially expressed proteins revealed that many significantly enriched GO terms were related to *extracellular matrix* (10^{-6} FDR) and *adhesion* (10^{-5} FDR) in the PPP vs. 3PH comparison (Fig. 3B), and to a lesser extent in the PHP vs. 3PH comparison (10^{-3} FDR for *ECM* and 10^{-4} FDR for *adhesion*) (suppl Fig. 3D). Among the differentially expressed proteins belonging to these GO categories we found collagens such as COL12A1, COL14A1, COL15A1, or hyaluronan-binding proteins such as TNFAIP6 or HAPLN1 (suppl Table 1), all of which were upregulated in both comparisons. By contrast, *ECM* and *adhesion* proteins were not differentially expressed in the PPP vs. PHP comparison (Fig. 3C). Of note, the
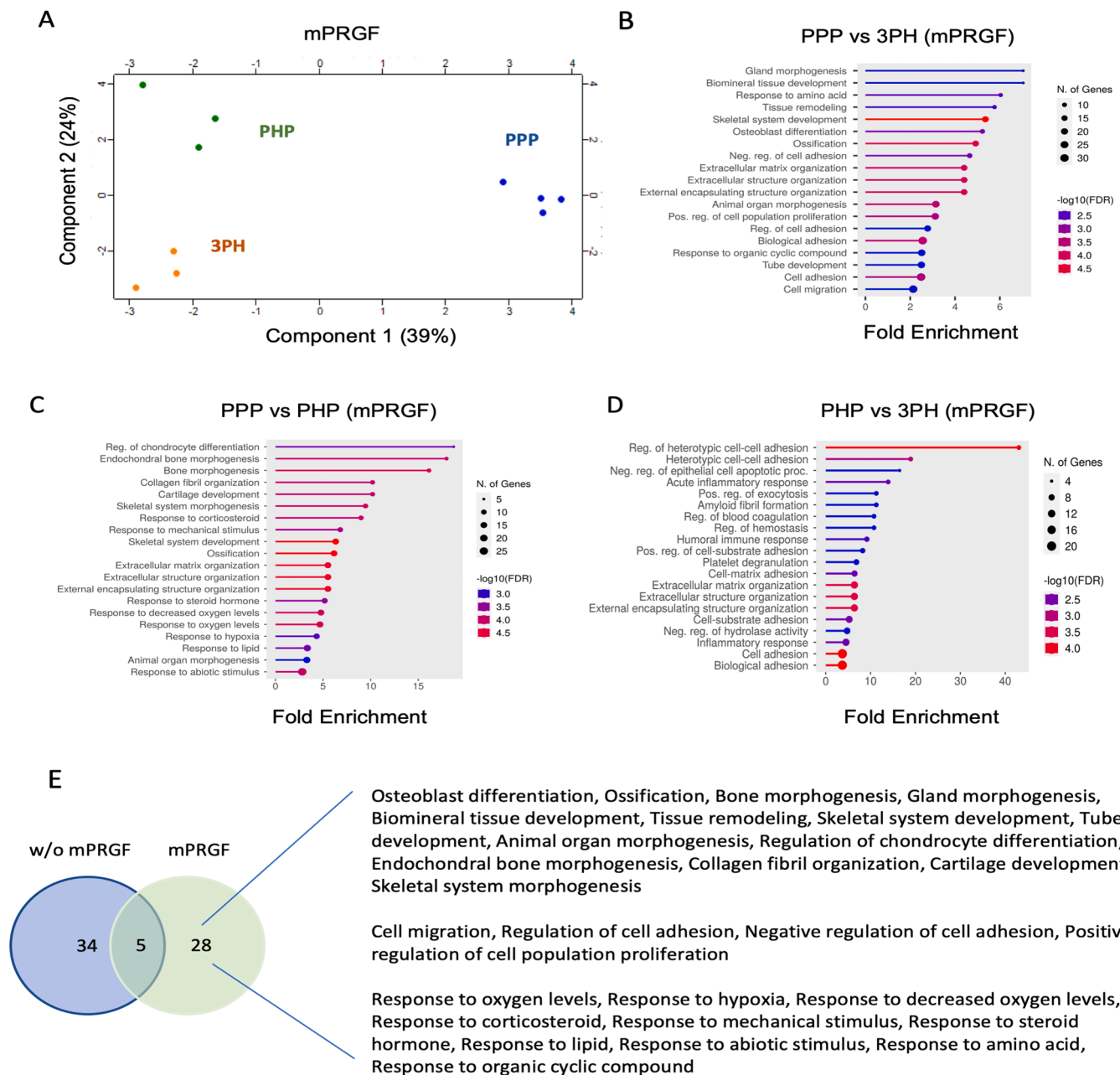
Fig. 4. Proteomic analysis of the triple-layered constructs with mPRGF. A) Principal component analysis (PCA) of proteomics data (Log2 fold changes) obtained in triple-layered constructs (n = 3). The PCA plot represents 6247 proteins with biological replicates that indicate proteomics profile differences between triple-layered constructs. B, C, D) Results of the GO enrichment analysis performed with the ShinyGO application, using as a background the total number of proteins identified in each of the comparisons. Shown are the number of differentially expressed proteins as spots belonging to top hallmark pathways. The spot size represents the number of differentially expressed proteins and spot color indicates enrichment confidence (FDR). X-axis denotes the enrichment factor of differentially expressed proteins. E) Venn diagram to compare all GO terms that are overrepresented in the PPP vs. 3PH and PPP vs. PHP comparisons between triple-layered constructs with or without fibrin.
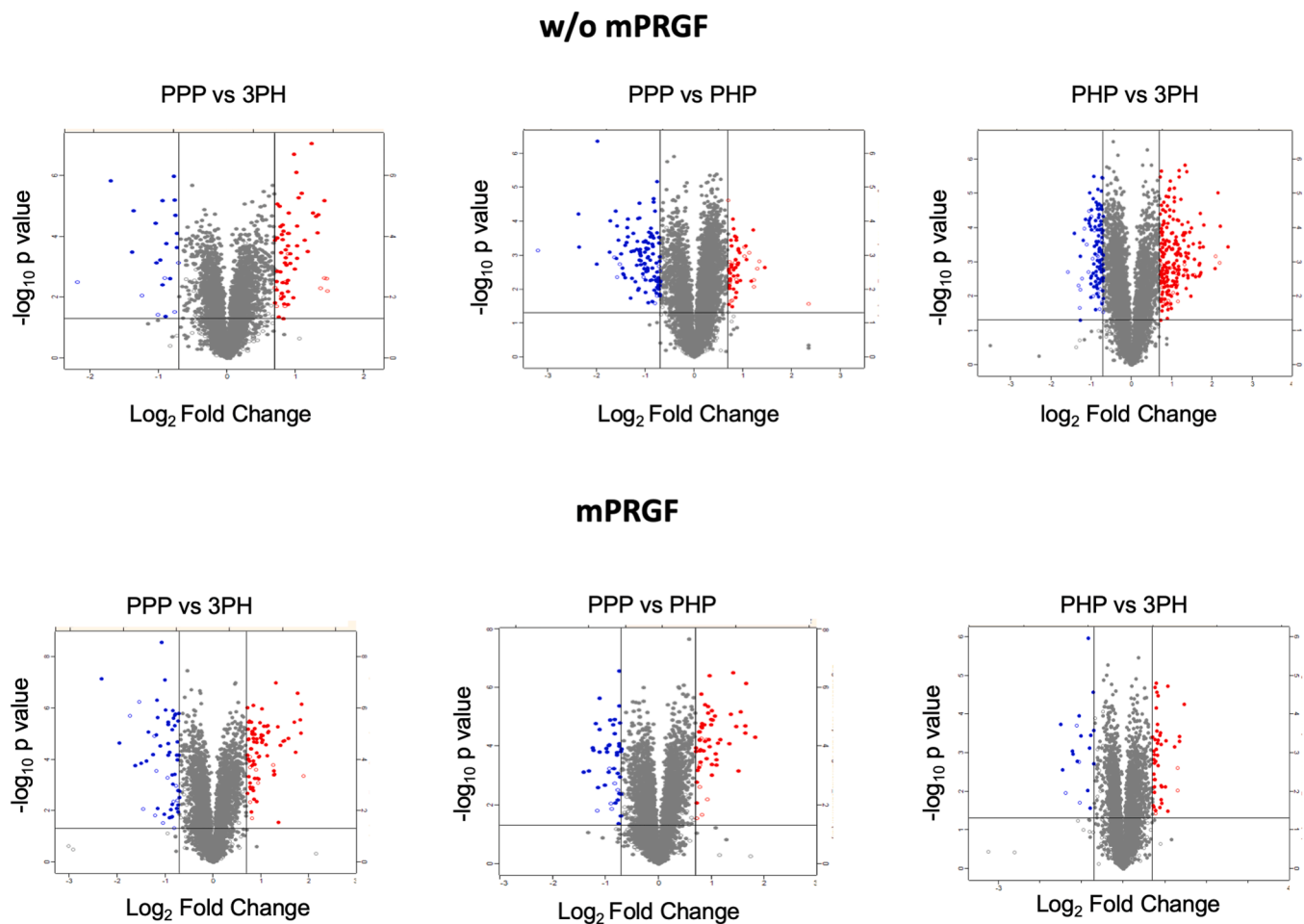
w/o mPRGF

mPRGF

Fig. 5. Volcano plot of protemic data, depicting protein data p-values *vs.* fold change between different constructs in the presence (mPRGF) and absence (w/o mPRGF) of the fibrin membrane. Red dots indicate differentially expressed proteins with log2 Fold Change > 0.7 and $p < 0.05$. Blue dots indicate differentially expressed proteins with log2 Fold Change < -0.7 and $p < 0.05$. ($n = 3$). Proteins are ranked according to their statistical p value (y-axis) as -log 10 and their relative abundance ratio (log 2 fold-change) (x-axis). Off-centered spots are those that vary the most between compared groups. Red dots indicate differentially expressed proteins with log2 Fold Change > 0.7 and $p < 0.05$. Blue dots indicate differentially expressed proteins with log2 Fold Change < -0.7 and $p < 0.05$.

sandwich configuration (PHP) exhibited a significant proportion of differentially expressed proteins related to coagulation and complement activation, which were absent in the PPP and 3PH configurations.

Regarding constructs with mPRGF, *ECM* and *adhesion* were also significantly enriched categories in PPP and PHP, particularly with the sandwich configuration (suppl Table 2). As in the situation without fibrin membrane, the 3PH configuration was the least favorable condition for *ECM* and *adhesion* protein expression relative to the other two constructs (Fig. 4). Remarkably, the inclusion of mPRGF led to the enrichment of new categories in the proteome of PPP constructs. In particular, the PPP configuration exhibited an overrepresentation of terms related to *osteogenesis*, *morphogenesis* and *development* that were absent in 3PH or PHP (Fig. 4, B and C). Most proteins included in these terms appeared upregulated in PPP. Additionally, proteins included in categories related to *hypoxia* appeared significantly downregulated in the PPP proteome compared to PHP.

To avoid a possible assessment bias emanating from the comparison of cell sheets that are constructed by two cell types (hPDLSC and HUVEC) cultured in different proportions, we analyzed the same type of constructs by comparing their proteomes in the presence or absence of mPRGF. For this analysis, GO data from PPP vs. PHP and from PPP vs. 3PH were used (Fig. 4E). Remarkably, the inclusion of mPRGF in the PPP constructs led to the emergence of 28 GO categories that were absent in cultures without mPRGF (suppl Tables 1, 2). These categories were related to *ossification, bone and cartilage morphogenesis* (for example

COL1A1, BMP6, VCAN, ITGA5 or RUNX), *cell proliferation* (CDKN1B, BCL2L1, MDK), *adhesion* (ICAM1, TNC, SNED1) *response to hormone* (PPAP2A, FOS, ALPL) and to *hypoxia* (ERO1L, PLOD2, CXCL12). The expression of most proteins included in these terms was upregulated in the mPRGF samples compared to samples without these PRGF membranes, with the exception of hypoxia-related proteins, which were downregulated, suggesting that the PPP+mPRGF configuration is the most favorable condition for regenerative purposes.

3.5. Detection of necrosis and glucose consumption

After culturing the 6 models of triple-layered cell constructs for 48 h, the metabolic state of the cells included in the triple-layered constructs was analyzed. Glucose consumption was found significantly elevated in the three composites with mPRGF. By contrast, the lowest glucose reduction was observed in the conditioned culture medium derived from the sandwiched constructs (PHP) without mPRGF (Fig. 6A). Moreover, LDH activity values were in accordance with the metabolic activity exhibited by the constructs, since the highest values were detected for the constructs showing the lowest glucose consumption (Fig. 6B), suggesting a higher rate of cell death in these configurations.

3.6. Quantification of biomolecules in the culture medium

The levels of the proteins associated to ECM fibronectin and type I
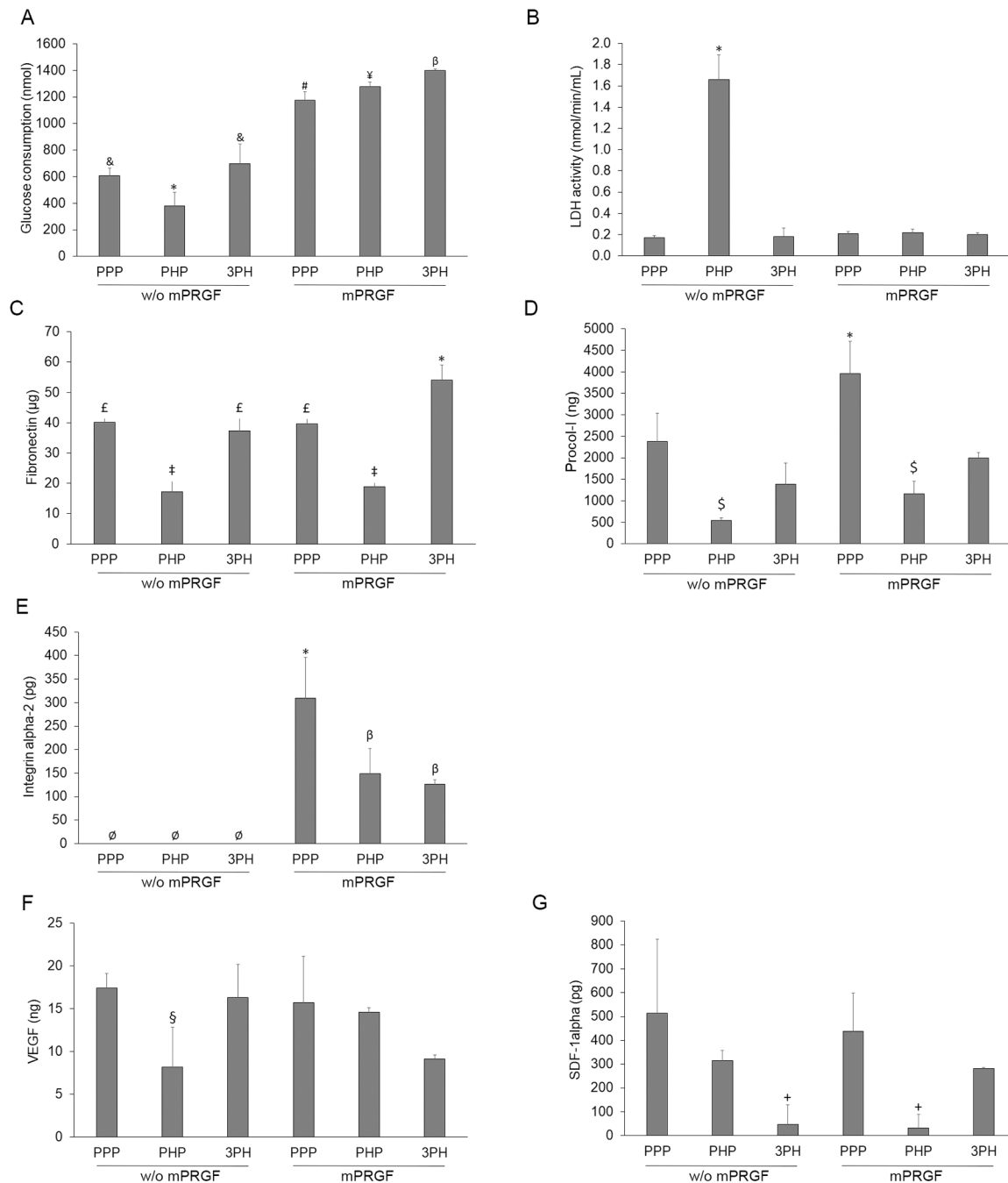
Fig. 6. Protein synthesis by triple-layered cell constructs and assessment of cell constructs viability and integrity after culturing for 48 h. A) Glucose consumption. *Statistically significant differences respect to PPP without mPRGF ($p < 0.05$) and to 3PH without mPRGF ($p < 0.01$) and to PPP, PHP and 3PH with mPRGF ($p < 0.001$). &Statistically significant differences respect to PHP without mPRGF ($p < 0.05$) and to PPP, PHP and 3PH with mPRGF ($p < 0.001$). #Statistically significant differences respect to PPP, PHP and 3PH without mPRGF ($p < 0.001$) and to 3PH with mPRGF ($p < 0.05$). ¥Statistically significant differences in comparison with PPP, PHP and 3PH without mPRGF ($p < 0.001$). βStatistically significant differences comparing to PPP, PHP and 3PH without mPRGF ($p < 0.001$) and to PPP with mPRGF ($p < 0.05$). B) Lactate dehydrogenase cell activity. *Statistically significant differences respect to the remaining constructs ($p \leq 0.001$). C) Fibronectin. ‡Statistically significant differences respect to PPP and 3PH without mPRGF and to PPP and 3PH with mPRGF ($p < 0.001$). £Statistically significant differences compared to PHP without mPRGF and to PHP and 3PH with mPRGF ($p \leq 0.001$). *Statistically significant differences respect to the remaining constructs ($p \leq 0.001$). D) Type I procollagen. *Statistically significant differences respect to PPP without mPRGF ($p < 0.05$) and to PHP and 3PH without mPRGF and to PHP with mPRGF ($p < 0.01$) and to 3PH with mPRGF ($p < 0.05$). $Statistically significant differences respect to PPP without mPRGF ($p < 0.05$) and to PPP and 3PH with mPRGF ($p < 0.01$). E) Integrin-alpha 2. ØStatistically significant differences compared to PPP, PHP with mPRGF ($p < 0.01$) and to 3PH onto mPRGF ($p < 0.001$). *Statistically significant differences respect to PPP, PHP and 3PH without mPRGF ($p < 0.01$) and to PHP and 3PH with mPRGF ($p < 0.05$). βStatistically significant differences comparing to PPP, PHP and 3PH without mPRGF ($p < 0.01$) and to PPP with mPRGF ($p < 0.05$). F) Vascular endothelial growth factor. §Statistically significant differences compared with PPP without mPRGF ($p < 0.05$). G) Stromal Cell Derived Factor-1 alpha. +Statistically significant differences respect to PHP without mPRGF and to PPP and 3PH with mPRGF ($p < 0.05$). Data are presented as mean ± SD ($n = 3$). Triple-layered cell constructs: PPP: hPDLSCs / hPDLSCs / hPDLSCs; PHP: hPDLSCs / HUVEC / hPDLSCs; 3PH: hPDLSCs:HUVEC / hPDLSCs:HUVEC / hPDLSCs:HUVEC. w/o mPRGF: without mPRGF; mPRGF: with mPRGF.

procollagen were quantified in the conditioned culture medium. A significantly higher level of fibronectin secreted by 3PH constructs onto mPRGF was detected, comparing to the remaining structures (Fig. 6C). On the contrary, the lowest fibronectin concentration was found in the conditioned media of PHP constructs both with and without fibrin membrane, being these differences statistically significant. Regarding

procollagen, the best results were achieved for the triple-layered composite constructs of hPDLSCs onto mPRGF, and statistically significant values were detected for this structure relative to all other three-layer models (3963±746 vs. 2381±657, 538±69, 1386±496, 1169±282 and 1999±120 for PPP composites onto mPRGF vs. fibrin free PPP, PHP and 3PH constructs, and for the structures lying on mPRGF consisting in
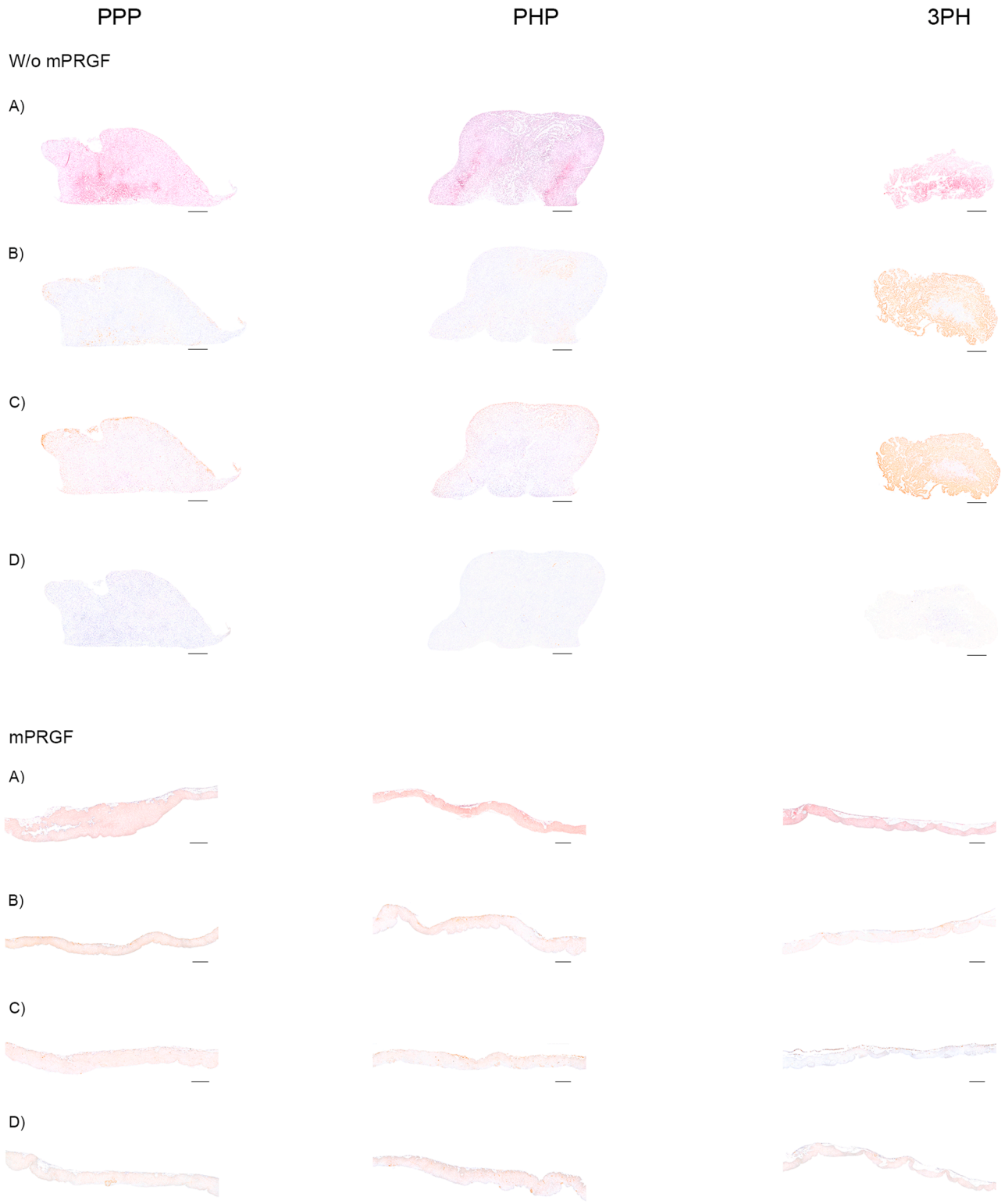
Fig. 7. Representative light microscope micrographs of triple-layered cell constructs cultured for 48 h. A) Haematoxylin and Eosin staining. B) collagen type I immunolabelling. C) TUNEL chromogenic apoptosis labelling. D) CD-31 immunolabelling (scale bar: 200 μm) (n = 3).

PHP and 3PH constructs, respectively) (Fig. 6D).

The quantification of integrin alpha-2 in the conditioned culture media by constructs was also carried out. The release of this cell adhesion protein was only detectable for triple-layered constructs onto mPRGF, with the highest concentration in the case of the hPDLSCs' composite constructs (310 ± 87 vs. 149 ± 53 and 126 ± 11 for 3D-structures of PPP vs. PHP and 3PH, respectively) (Fig. 6E), in line with proteomic results.

The concentration of VEGF and SDF-1α proteins was also determined. None of the constructs showed statistically significant differences in their secretion into the culture medium or in the cellular proteome. However, regarding SDF-1α, both the conditioned media of 3PH without mPRGF and PHP construct onto mPRGF showed significantly lower levels relative to the rest of the constructs, except for the hPDLSCs triple-layered composite without mPRGF (Fig. 6, F and G).

3.7. Histological analysis

At the histological level, PPP and PHP constructs showed similar morphological features, collagen type I distribution patterns and extent of cell death on the peripheral area. Nevertheless, CD31 could only be detected in triple-layered cell constructs of PHP. By contrast, 3PH constructs showed a more complex structural organization, with individual cell layers, irregular edges and a looser core area. Moreover, collagen type I and apoptosis were spread much more widely, with the exception of the inner part of the constructs (Fig. 7). When triple-layered cell sheets were cultured on PRGF membranes, PHP seemed to synthesize more collagen type I and CD31 compared to the other constructs, in line with proteomic results.

4. Discussion

ECM comprises a highly complex and dynamic 3D network that provides support and regulates cell behaviour, phenotype and function [43,44], thus becoming pivotal in wound healing [45]. CST technology avoids proteolytic enzyme treatment for cell detachment, thereby preserving efficiently cell-cell junctions and ECM. In addition, this conservation of ECM integrity favours the adhesion to injured tissue without the need of sutures or external fixation [2,46]. However, due to the detaching process, a cytoskeletal reorganization occurs, and cell sheets shrink significantly. To overcome this size reduction, cell sheets can be used in combination with different scaffolds. Here we report the use of autologous PRGF technology to obtain a fibrin membrane that prevents this surface shrinkage, facilitates handling, improves the weak mechanical support of cell sheets alone and provides biological cues that are essential for tissue regeneration [2,46].

Ensuring vascularization is one of the main challenges of tissue engineering since its absence leads to tissue necrosis and failure of construct implantation [47]. Several approaches have been attempted to achieve successful vascularization, including coculturing of MSCs and endothelial cells, as progenitor cells could promote prevascularised networks [48]. When it comes to cell layering, construct thickness is limited by the successfully diffusion of oxygen and nutrients [49,50]. Therefore, endothelial cells have been included in our 3D constructs, either as constituents of co-cultures or as sandwiched cell sheets to assess their impact on the engineered tissues. However, our data show that the presence of HUVEC does not improve cellular metabolism, represented by glucose consumption or by responses to hypoxia. Instead, the sandwich configuration PHP is the construct with the lowest glucose consumption, and this HUVEC-containing construct exhibited higher levels of hypoxia-related proteins compared to the PPP configuration. Along these lines, significantly higher values of cell death were detected in the sandwiched triple-layer constructs without mPRGF. These higher levels of cell death would be behind the statistically significant lower glucose consumption in this type of construct. The way in which this sandwiched triple-layer structure was constructed may have influenced

the results, as the HUVEC cell sheet was fragmented and subjected to an extra centrifugation process before being placed between the two periodontal ligament stem cell sheets. However, these higher levels of cell death were completely absent when mPRGF was included in the construct composition, an autologous membrane with a porous structure and a plethora of biological cues involved in physiological processes, such as cell proliferation and differentiation [37,51–53].

Healing and tissue formation are largely dependent on the ECM, which is composed of a complex 3D interconnecting network of glycosaminoglycans (GAGs) and proteins [43,54]. According to our proteomic data, the inclusion of a layer of HUVEC cells did not negatively affect the capacity of hPDLSC cells to express proteins that are important for the extracellular structure organization of the constructs, whereas the coculture configuration was clearly less favorable with regard to ECM and adhesion molecule production. Furthermore, the secretion of ECM related proteins, including fibronectin, type I procollagen and ITG-α2 was lower in the sandwiched triple-layer structures regardless of the inclusion of mPRGF, thus indicating a poor performance of these types of constructs.

ECM is known to be crucial for angiogenesis, by supplying cell signals that promote vessel formation and maturation [47,55,56]. In this sense, CST provides an excellent microenvironment for vascularization as the ECM remains intact [50]. As summarized by Karamysheva, there are several factors that play a critical role during angiogenesis [57]. VEGF is the most specific and potent angiogenic factor whereas SDF-1 is a chemokine that promotes the recruitment of stem and progenitor cells, including endothelial progenitor cells [58–60]. Thus, a combination of both factors exhibits synergistic properties on angiogenesis [60]. Regarding these angiogenic factors, the results obtained in this study did not show clear differences among the different constructs. In fact, only in the case of SDF-1α, the groups PHP and 3PH, both with and without mPRGF, exhibited statistically lower synthesis. Therefore, the inclusion of endothelial cells did not clearly enhance the VEGF- and SDF-1α-mediated vascularisation of these constructs. The preservation of the intact extracellular matrix, an advantage derived from the use of CST, and in some cases the inclusion of mPRGF, is probably sufficient to stimulate the synthesis of these angiogenic factors and may even outweigh the effect of endothelial cell inclusion. The complex multistep process of angiogenesis requires several cell types, ECM components, growth factors and cytokines [47]. In this sense, fibrin is one of the native ECM components that provides a plethora of growth factors and proteins involved in the tissue regeneration process, including new vascular networks [55,61]. In this sense, it would be useful to evaluate, in future assays, the vascularization capacity of these constructs *in vivo*, to confirm whether the inclusion of endothelial cells is really dispensable in these types of constructs.

ECM proteins closely determine cells' dynamic and behaviour including cell adhesion, migration, proliferation, differentiation, and apoptosis [13,43]. ECM also provides the main mechanical support, architecture and strength for tissues and regulates cell phenotype [44, 45]. Therefore, preserving the ECM and enhancing its formation is critical for the complete regeneration of the damaged tissue [13]. The data reported in this article suggest that mPRGF could increase cell matrix production, as the highest levels of ECM-related proteins were detected in constructs cultured onto mPRGF. More specifically, the triple-layered construct of hPDLSCs showed the highest synthesis of collagen and integrin α2, while the greatest levels of fibronectin were determined in the 3PH group. Our proteomic data confirmed the superior properties of constructs carrying a fibrin scaffold. This ability of the PRGF formulations to stimulate different biological processes, including the synthesis of diverse components of the extracellular matrix, has been extensively described previously in these and other cell phenotypes [35, 51,52,62].

CST has been applied to many different tissues such as heart, liver, cornea, bladder, oesophagus, bone, thyroid and periodontium [50,63]. However, it also shows some limitations, including the spontaneous

contraction and the low mechanical properties of cell sheets, which need to be solved. Combining this technology with scaffolds has been proposed to overcome these shortcomings and to turn it into a more feasible strategy [2,3,64]. In fact, Lesman et al. [65] reported an increase in the mechanical strength of the 3D fibrin-based constructs. Similarly, Iwata et al. [66] showed the safety and efficacy of autologous three-layered periodontal ligament-derived cell sheets in severe periodontal defects. These data are consistent with our study, where the best construct was the one composed of a triple-layered of periodontal ligament stem cells. Other authors [13,67] have reported that the inclusion of bone-derived cells along with periodontal ligament cells showed a better performance, that is, complex cell sheets composed of two related tissues provided a more suitable microenvironment for the regeneration of periodontal tissue defects. On the other hand, and in contrast to the findings reported in our study, several authors have shown that the inclusion of HUVECs in cell sheet constructs has a positive impact [63,68,69]. Nevertheless, differences in the experimental design, such as cell density, number of layers or co-culture conditions, may be behind this disparity in results. Therefore, and given the importance of developing a cross-cutting strategy that provides prevascularised networks, further in-depth studies will be a line of work to determine the involvement of HUVECs, in order to achieve an efficient therapeutic protocol for developing an optimum 3D cell sheet-based approach. Moreover, multilayer human dental pulp stem cell (hDPSC) sheets supplied with vitamin C have been also reported to produce enhanced bone regeneration and promising therapeutic results when transplanted to the bone defect location in a periodontitis swine model [70,71]. *In vivo* experiments revealed that a sandwich structure of vitamin C induced hDPSCs, human dentin matrix (hTDM) and Matrigel promoted the regeneration of a periodontium-like dense connective tissue around the hTDM, together with the formation of a great mass of predentin on the cavity side of hTDM, and the emergence of odontoblast-like cells, blood vessel-like structures and nerve-like fibers in the pulp cavity [72,73]. The use of engineered cell sheets containing human MSCs and stem cells from human exfoliated deciduous teeth (SHEDs) for repairing cleft palate and also for regenerating palatal bone has been explored [74]. According to Nam et al., submandibular gland (SMG) based thermoresponsive cell sheets could preserve secretory granules and cell–cell junctions, whereas double-layered cell sheets, could promote tissue formation, cell differentiation, saliva secretion and submandibular gland repair in a wounded SMG murine model [75].

In summary, the preliminary results obtained in this study showed that the inclusion of mPRGF aided the formation of cell sheets, by preventing their shrinkage and therefore enabling their handling. By contrast, the inclusion of HUVECs did not clearly improve the biological properties of these constructs but made them more difficult to handle. Importantly, mPRGF positively influenced the cellular behaviour thus stimulating metabolic activity and increasing matrix synthesis. At the proteome level, the inclusion of a mPRGF membrane conferred a dramatic advantage to the hPDLSCs triple-layered constructs in their ability to provide a suitable environment for tissue regeneration, as mPRGF stimulated the production of proteins that are necessary for osteogenic differentiation and cellular proliferation, among others. Overall, these results suggest the suitability of hPDLSCs triple-layer constructs for regenerative purposes and feature mPRGF as a promising tool to support cell sheet formation and handling and to improve their biological functions.

Ethics approval

The study was performed following the principles established in the Declaration of Helsinki amended in 2013 and in accordance with the ethical standards from the Araba University Hospital Clinical Research Ethical Committee (BTI-01-IV/02/20/CST). Informed consent was obtained from all individual participants included in the study.

Authors' contribution

E.A., M.Z., M.T., A.Z., A.F., and M.H.A. have made substantial contributions to conception and design of the study. M.T., M.Z., R.T. and N. O. carried out the experiments. All authors have been involved in data interpretation, drafting and revising critically the manuscript. All authors have read and given final approval of the version to be published.

Funding

Competing interest

The authors declare the following competing financial interests: E.A. is the Scientific Director of and M.T, M.Z., R.T., and M.H.A. are scientists at BTI Biotechnology Institute, a dental implant company that investigates in the fields of oral implantology and PRGF-Endoret technology. N.O., A.F. and A.M.Z. declare no conflict of interest.

Appendix A. Supporting information

Supplementary data associated with this article can be found in the online version at doi:10.1016/j.biopha.2024.116599.

References

[1] M. Li, J. Ma, Y. Gao, L. Yang, Cell sheet technology: a promising strategy in regenerative medicine, Cytotherapy 21 (1) (2019) 3–16.

[2] Y. Lu, et al., Recent advances in cell sheet technology for bone and cartilage regeneration: from preparation to application, Int J. Oral. Sci. 11 (2) (2019) 17.

[3] I.M. Zurina, V.S. Presniakova, D.V. Butnaru, A.A. Svistunov, P.S. Timashev, Y. A. Rochev, Tissue engineering using a combined cell sheet technology and scaffolding approach, Acta Biomater. 113 (2020) 63–83.

[4] N. Matsuda, T. Shimizu, M. Yamato, T. Okano, Tissue engineering based on cell sheet technology, Adv. Mater. 19 (20) (2007) 3089–3099.

[5] M. Yamato, T. Okano, Cell sheet engineering, Mater. Today 7 (5) (2004) 42–47.

[6] D. Chang, et al., Time course of cell sheet adhesion to porcine heart tissue after transplantation, PLoS One 10 (10) (2015) e0137494.

[7] J. Kobayashi, A. Kikuchi, T. Aoyagi, T. Okano, Cell sheet tissue engineering: Cell sheet preparation, harvesting/manipulation, and transplantation, J. Biomed. Mater. Res A 107 (5) (2019) 955–967.

[8] P. Thummarati, W. Laiwattanapaisal, R. Nitta, M. Fukuda, A. Hassametto, M. Kino-Oka, Recent advances in cell sheet engineering: from fabrication to clinical translation, Bioengineering 10 (2) (2023).

[9] C. Pu, R. Lin, S. Liang, X. Qiu, H. Hou, Smart surface-based cell sheet engineering for regenerative medicine, Trends Chem. 5 (1) (2023) 88–101.

[10] C. Imashiro, T. Shimizu, Fundamental Technologies and Recent Advances of Cell-Sheet-Based Tissue Engineering, Int J. Mol. Sci. 22 (1) (2021).

[11] A. Shahin-Shamsabadi, J. Cappuccitti, Anchored cell sheet engineering: a novel scaffold-free platform for in vitro modeling, Adv. Funct. Mater. 2308552 (2023).

[12] D. Hu, et al., The preclinical and clinical progress of cell sheet engineering in regenerative medicine, Stem Cell Res Ther. 14 (1) (2023) 112.

[13] H. Zhang, S. Liu, B. Zhu, Q. Xu, Y. Ding, Y. Jin, Composite cell sheet for periodontal regeneration: crosstalk between different types of MSCs in cell sheet facilitates complex periodontal-like tissue regeneration, Stem Cell Res Ther. 7 (1) (2016) 168.

[14] T. Kikuchi, T. Shimizu, M. Wada, M. Yamato, T. Okano, Automatic fabrication of 3-dimensional tissues using cell sheet manipulator technique, Biomaterials 35 (8) (2014) 2428–2435.

[15] Y. Haraguchi, et al., Fabrication of functional three-dimensional tissues by stacking cell sheets in vitro, Nat. Protoc. 7 (5) (2012) 850–858.

[16] K. Nagase, M. Yamato, H. Kanazawa, T. Okano, Poly(N-isopropylacrylamide)-based thermoresponsive surfaces provide new types of biomedical applications, Biomaterials 153 (2018) 27–48.

[17] Kanai N., Yamato M., Okano T. (2014) Principles of Cell Sheet Technology.57-66.

[18] Y. Han, X. Li, Y. Zhang, Y. Han, F. Chang, J. Ding, Mesenchymal Stem Cells for Regenerative Medicine, Cells 8 (8) (2019).

[19] M. Merimi, et al., The Therapeutic Potential of Mesenchymal Stromal Cells for Regenerative Medicine: Current Knowledge and Future Understandings, Front. Cell Dev. Biol. 9 (2021).

[20] C. Brown, et al., Mesenchymal stem cells: Cell therapy and regeneration potential, J. Tissue Eng. Regen. Med. 13 (9) (2019) 1738–1755.

[21] O. Trubiani, et al., Periodontal Ligament Stem Cells: Current Knowledge and Future Perspectives, Stem Cells Dev. 28 (15) (2019) 995–1003.

[22] J. Chen, et al., The application of human periodontal ligament stem cells and biomimetic silk scaffold for in situ tendon regeneration, Stem Cell Res. Ther. 12 (1) (2021) 596.

[23] D.S. Masson-Meyers, L. Tayebi, Vascularization strategies in tissue engineering approaches for soft tissue repair, J. Tissue Eng. Regen. Med 15 (9) (2021) 747–762.

[24] E. Novosel, C. Kleinhans, P. Kluger, Vascularization is the key challenge in tissue engineering, Adv. Drug Deliv. Rev. 63 (2011) 300–311.

[25] A. Alghuwainem, A.T. Alshareeda, B. Alsowayan, Scaffold-Free 3-D Cell Sheet Technique Bridges the Gap between 2-D Cell Culture and Animal Models, Int J. Mol. Sci. 20 (19) (2019).

[26] A.C. Brown, T.H. Barker, Fibrin-based biomaterials: modulation of macroscopic properties through rational design at the molecular level, Acta Biomater. 10 (4) (2014) 1502–1514.

[27] K.L. Christman, Biomaterials for tissue repair, Science 363 (6425) (2019) 340–341.

[28] E. Anitua, M. Fuente, F. Muruzabal, J. Merayo-Lloves, Development and optimization of a personalized fibrin membrane derived from the plasma rich in growth factors technology, Exp. Eye Res 203 (2021) 108402.

[29] E. Anitua, F. Muruzabal, M. de la Fuente, S. Del Olmo-Aguado, M.H. Alkhraisat, J. Merayo-Lloves, PRGF Membrane with Tailored Optical Properties Preserves the Cytoprotective Effect of Plasma Rich in Growth Factors: In Vitro Model of Retinal Pigment Epithelial Cells, Int J. Mol. Sci. 24 (13) (2023).

[30] E. Anitua, M. Zalduendo, M. Troya, R. Tierno, M.H. Alkhraisat, Cellular composition modifies the biological properties and stability of platelet rich plasma membranes for tissue engineering, J. Biomed. Mater. Res A 111 (11) (2023) 1710–1721.

[31] R.M. Sánchez-Ávila, et al., Fibrin-Plasma Rich in Growth Factors Membrane for the Treatment of a Rabbit Alkali-Burn Lesion, Int J. Mol. Sci. 22 (11) (2021).

[32] I. Rodríguez-Agirretxe, V. Freire, F. Muruzabal, G. Orive, E. Anitua, E. Díez-Feijóo, A. Acera, Subconjunctival PRGF Fibrin Membrane as an Adjuvant to Nonpenetrating Deep Sclerectomy: A 2-Year Pilot Study, Ophthalmic Res 59 (1) (2018) 45–52.

[33] R.M. Sanchez-Avila, et al., Plasma rich in growth factors membrane as coadjuvant treatment in the surgery of ocular surface disorders, Med. (Baltim.) 97 (17) (2018) e0242.

[34] E. Anitua, F. Muruzabal, M. de la Fuente, J. Merayo-Lloves, M.H. Alkhraisat, Development of a new plasma rich in growth factors membrane with improved optical properties, Ann. Anat. 248 (2023) 152071.

[35] E. Anitua, M. Troya, G. Orive, An autologous platelet-rich plasma stimulates periodontal ligament regeneration, J. Periodo 84 (11) (2013) 1556–1566.

[36] M. Dominici, et al., Minimal criteria for defining multipotent mesenchymal stromal cells. The International Society for Cellular Therapy position statement, Cytotherapy 8 (4) (2006) 315–317.

[37] E. Anitua, M. Zalduendo, M. Troya, Autologous plasma rich in growth factors technology for isolation and ex vivo expansion of human dental pulp stem cells for clinical translation, Regen. Med. 14 (2) (2019) 97–111.

[38] J.R. Wiśniewski, A. Zougman, N. Nagaraj, M. Mann, Universal sample preparation method for proteome analysis, Nat. Methods 6 (5) (2009) 359–362.

[39] S. Tyanova, T. Temu, J. Cox, The MaxQuant computational platform for mass spectrometry-based shotgun proteomics, Nat. Protoc. 11 (12) (2016) 2301–2319.

[40] S. Tyanova, et al., The Perseus computational platform for comprehensive analysis of (prote)omics data, Nat. Methods 13 (9) (2016) 731–740.

[41] S.X. Ge, D. Jung, R. Yao, ShinyGO: a graphical gene-set enrichment tool for animals and plants, Bioinformatics 36 (8) (2020) 2628–2629.

[42] P. Bardou, J. Mariette, F. Escudié, C. Djemiel, C. Klopp, jvenn: an interactive Venn diagram viewer, BMC Bioinforma. 15 (1) (2014) 293.

[43] D.L. Kusindarta, H. Wihadmadyatami, The Role of Extracellular Matrix in Tissue Regeneration, Tissue Regen. (2018).

[44] L. Salvatore, N. Gallo, M.L. Natali, A. Terzi, A. Sannino, M. Madaghiele, Mimicking the Hierarchical Organization of Natural Collagen: Toward the Development of Ideal Scaffolding Material for Tissue Regeneration, Front. Bioeng. Biotechnol. 9 (2021).

[45] Z. Mackiewicz, Y.T. Konttinen, E. Peltola, V. Stegajev, H.D. Wagner, J. Levon, V. M. Tiainen, Extracellular matrix and tissue regeneration, Book Title (2016).

[46] A. De Pieri, Y. Rochev, D.I. Zeugolis, Scaffold-free cell-based tissue engineering therapies: advances, shortfalls and forecast, npj Regen. Med. 6 (1) (2021) 18.

[47] S.V. Lopes, M.N. Collins, R.L. Reis, J.M. Oliveira, J. Silva-Correia, Vascularization approaches in tissue engineering: recent developments on evaluation tests and modulation, ACS Appl. Bio Mater. 4 (4) (2021) 2941–2956.

[48] L. Ren, D. Ma, B. Liu, J. Li, J. Chen, D. Yang, P. Gao, Preparation of three-dimensional vascularized MSC cell sheet constructs for tissue regeneration, Biomed. Res Int 2014 (2014) 301279.

[49] W. Sekine, Y. Haraguchi, T. Shimizu, A. Umezawa, T. Okano, Thickness limitation and cell viability of multi-layered cell sheets and overcoming the diffusion limit by a porous-membrane culture insert, J. Biochip Tissue Chip S 1 (2011) (2153-0777).

[50] K. Moschouris, N. Firoozi, Y. Kang, The application of cell sheet engineering in the vascularization of tissue regeneration, Regen. Med. 11 (6) (2016) 559–570.

[51] E. Anitua, M. Troya, M. Zalduendo, R. Tejero, G. Orive, Progress in the Use of Autologous Regenerative Platelet-based Therapies in Implant Dentistry, Curr. Pharm. Biotechnol. 17 (5) (2016) 402–413.

[52] E. Anitua, M.M. Sanchez, M. de la Fuente, R. Prado, G. Orive, I. Andia, Fibroblastic response to treatment with different preparations rich in growth factors, Cell Prolif. 42 (2) (2009) 162–170.

[53] E. Anitua, M. Sanchez, J. Merayo-Lloves, M. De la Fuente, F. Muruzabal, G. Orive, Plasma rich in growth factors (PRGF-Endoret) stimulates proliferation and migration of primary keratocytes and conjunctival fibroblasts and inhibits and reverts TGF-beta1-Induced myodifferentiation, Invest Ophthalmol. Vis. Sci. 52 (9) (2011) 6066–6073.

[54] M. Assunção, D. Dehghan-Baniani, C.H.K. Yiu, T. Später, S. Beyer, A. Blocki, Cell-Derived Extracellular Matrix for Tissue Engineering and Regenerative Medicine, Front. Bioeng. Biotechnol. 8 (2020).

[55] S.A. Ishak, J.R.P. Djuansjah, M.R.A. Kadir, I. Sukmana, Angiogenesis in tissue engineering: from concept to the vascularization of scaffold construct, IOP Conf. Ser.: Mater. Sci. Eng. 58 (2014) 012015.

[56] Y. Wang, et al., Extracellular matrix sheet modified with VEGF-loaded nanoparticles for bladder regeneration, NPG Asia Mater. 14 (1) (2022).

[57] A.F. Karamysheva, Mechanisms of angiogenesis, Biochemistry 73 (7) (2008) 751–762.

[58] F. Jin, N. Hagemann, S.T. Schafer, U. Brockmeier, A. Zechariah, D.M. Hermann, SDF-1 restores angiogenesis synergistically with VEGF upon LDL exposure despite CXCR4 internalization and degradation, Cardiovasc Res 100 (3) (2013) 481–491.

[59] F. Yang, F. Xue, J. Guan, Z. Zhang, J. Yin, Q. Kang, Stromal-Cell-Derived Factor (SDF) 1-Alpha Overexpression promotes bone regeneration by osteogenesis and angiogenesis in osteonecrosis of the femoral head, Cell Physiol. Biochem 46 (6) (2018) 2561–2575.

[60] Y. Cun, B. Diao, Z. Zhang, G. Wang, J. Yu, L. Ma, Z. Rao, Role of the stromal cell derived factor-1 in the biological functions of endothelial progenitor cells and its underlying mechanisms, Exp. Ther. Med. 21 (1) (2020).

[61] E. Anitua, M.H. Alkhraisat, G. Orive, Perspectives and challenges in regenerative medicine using plasma rich in growth factors, J. Control Release 157 (1) (2012) 29–38.

[62] E. Anitua, A. Pino, G. Orive, Plasma rich in growth factors promotes dermal fibroblast proliferation, migration and biosynthetic activity, J. Wound Care 25 (11) (2016) 680–687.

[63] C.P. Panduwawala, X. Zhan, W.L. Dissanayaka, L.P. Samaranayake, L. Jin, C. Zhang, In vivo periodontal tissue regeneration by periodontal ligament stem cells and endothelial cells in three-dimensional cell sheet constructs, J. Periodontal Res 52 (3) (2017) 408–418.

[64] Q. You, M. Lu, Z. Li, Y. Zhou, C. Tu, Cell Sheet Technology as an Engineering-Based Approach to Bone Regeneration, Int. J. Nanomed. Volume 17 (2022) 6491–6511.

[65] A. Lesman, J. Koffler, R. Atlas, Y.J. Blinder, Z. Kam, S. Levenberg, Engineering vessel-like networks within multicellular fibrin-based constructs, Biomaterials 32 (31) (2011) 7856–7869.

[66] T. Iwata, et al., Periodontal regeneration with autologous periodontal ligament-derived cell sheets – A safety and efficacy study in ten patients, Regen. Ther. 9 (2018) 38–44.

[67] R. Raju, et al., Three-dimensional periodontal tissue regeneration using a bone-ligament complex cell sheet, Sci. Rep. 10 (1) (2020) 1656.

[68] T. Sasagawa, T. Shimizu, S. Sekiya, Y. Haraguchi, M. Yamato, Y. Sawa, T. Okano, Design of prevascularized three-dimensional cell-dense tissues using a cell sheet stacking manipulation technology, Biomaterials 31 (7) (2010) 1646–1654.

[69] P.K. Pandula, L.P. Samaranayake, L.J. Jin, C.F. Zhang, Human umbilical vein endothelial cells synergize osteo/odontogenic differentiation of periodontal ligament stem cells in 3D cell sheets, J. Periodontal Res 49 (3) (2014) 299–306.

[70] D. Hu, et al., The preclinical and clinical progress of cell sheet engineering in regenerative medicine, Stem Cell Res. Ther. 14 (1) (2023) 112.

[71] F. Wei, et al., Vitamin C treatment promotes mesenchymal stem cell sheet formation and tissue regeneration by elevating telomerase activity, J. Cell Physiol. 227 (9) (2012) 3216–3224.

[72] H. Meng, L. Hu, Y. Zhou, Z. Ge, H. Wang, C.T. Wu, J. Jin, A Sandwich Structure of Human Dental pulp stem cell sheet, treated dentin matrix, and matrigel for tooth root regeneration, Stem Cells Dev. 29 (8) (2020) 521–532.

[73] R. Li, et al., Human treated dentin matrix as a natural scaffold for complete human dentin tissue regeneration, Biomaterials 32 (20) (2011) 4525–4538.

[74] J.M. Lee, et al., Developing palatal bone using human mesenchymal stem cell and stem cells from exfoliated deciduous teeth cell sheets, J. Tissue Eng. Regen. Med 13 (2) (2019) 319–327.

[75] K. Nam, K. Kim, S.M. Dean, C.T. Brown, R.S. Davis, T. Okano, O.J. Baker, Using cell sheets to regenerate mouse submandibular glands, npj Regen. Med. 4 (1) (2019) 16.